Research Square

Preprints are preliminary reports that have not undergone peer review.
They should not be considered conclusive, used to inform clinical practice,
or referenced by the media as validated information.

Novel synthesis and characterization of gold-platinum core-shell nanoparticles using green tea leaves extract

Le Thi Mai Hoa

lehoa2012fr@gmail.com

Vietnam National University Ho Chi Minh City

Research Article

Keywords: Core-shell nanoparticles, green synthesis, spherical morphology

Posted Date: April 8th, 2026

DOI: https://doi.org/10.21203/rs.3.rs-9281171/v1

License: This work is licensed under a Creative Commons Attribution 4.0 International License.
Read Full License

Additional Declarations: No competing interests reported.

Abstract

In the current study, core-shell Au-Pt nanoparticles (Au@Pt NPs) have been successfully synthesized via a new, facile and environmentally friendly approach, in which a Pt shell grown on an Au core surface by using green tea leaves extract as both a reducing and stabilization reagent. We have systematically studied the effects of the molar ratio between Au and Pt on the formation of the Au@Pt NPs. The molar ratio between Au and Pt is effectively controlled by changing the precursor solution ratios of $HAuCl_4$ and H_2PtCl_6 in the reaction solution, leading to controllable size. The surface morphology, crystalline structure and optical properties of the Au@Pt NPs are characterized by field emission scanning electron microscopy (FE-SEM) and X-ray diffraction (XRD), dynamic light scattering (DLS), UV-Vis spectroscopy. These results confirm that the Au@Pt nanoparticles are successfully prepared using a simple on-step method. The gold-platinum core-shell nanoparticles with molar ratio of (2:1) reveal good morphology, homogeneity in size and stability in comparison with the other synthesized Au@Pt NPs.

1. Introduction

Noble metallic nanoparticles have been of great scientific and significant attention owing to their exceptional physicochemical properties and play important roles for versatile applications in biomedical and pharmaceutical fields, electronics, environmental catalysis, fuel cells and energy storage [1–3]. The excellent properties of nanoparticles (NPs) depend not only on their morphologies and compositions but also on their structures and size [4, 5]. To date, the diverse morphologies of nanoparticles have been well regulated, including nanoflowers, nanorods, nanospheres [6–8]. Platinum (Pt) is well known due to its exceptional electrocatalytic properties, making them ideal for numerous applications [9, 10–13]. However, their low utilization efficiency and high cost poses particular difficulties for developing widespread applications [12–15]. Therefore, combining Pt with another element has recently been identified as a high effective approach to improve catalytic performance and optimize Pt utilization [13–16]. Among various metallic, gold (Au) is well known owing to its unique chemical stability, plasmonic properties and considered as an excellent metal to optimize the Pt utilization with core-shell nanostructure [17–19]. Gold is a less expensive noble metal than Pt. The synthesis of gold nanoparticles (AuNPs) is less difficult owing to the high reduction properties, making them suitable as a core material of core-shell nanoparticles [20]. The Pt shell, grown on the Au core surface, significantly forms a stable nanostructure due to strong electronic coupling between these two metal components [21–23]. The Au and Pt interaction exhibits synergistic effect owing to the alteration in Pt electronic band structure and further changes the specific surface area, which finally contributes to a significant enhancement of catalytic performance, electrochemical stability, efficiency and durability, making these nanoparticles highly attractive for widespread applications in biosensor, electrocatalytic, environmental remediation [21, 24–28]. In comparison to single metal nanoparticles, combining the unique properties of both Au and Pt, core-shell nanoparticles not only exhibit the unique physicochemical properties of the original metal core, but also have special surface features and electronic structures [25–27].

In recent years, core-shell nanoparticles composed of a gold core and a platinum shell (abbreviated as Au@Pt NPs) have been much investigated owing to their excellent catalytic performance for various catalytic reactions compared with those of Pt and Au nanoparticles [25–27]. However, a great challenge still remains is to control the deposition of Pt layers onto AuNPs substrates due to the lattice mismatch and occurrence of galvanic replacement reaction between Pt shell and Au core [17–19]. Therefore, various experimental methods have been employed to achieve the facile synthesis of Au@Pt NPs, and optimal core–shell size ratios have been explored in an effort to improve the catalytic activity and reduce the consumption of Pt [23, 26].

There have been many strategic routes have been applied to synthesize of core-shell Au-Pt nanoparticles, including ultrasonication, hydrothermal, sonochemical, galvanic replacement reaction (GRR) method [29, 33–37]. Ultrasonication method is commonly applied to generate high pressure and high temperature conditions that facilitate the reduction of Pt ions and NP formation [33, 38, 39]. Sonochemical method can be employed to accelerate and promote chemical reactions, including short reaction times, low reaction temperatures, rapid reaction rates [34]. The advantage of sonochemical approaches is to enable the synthesis of homogeneous and smaller nanoparticles. Seed-mediated methods are reported to be enabling precise control the core and shell morphology and size of Au@Pt NPs. A. Higareda and co-workers [7] present the synthesis of Au@Pt nanoparticles by using the galvanic replacement reaction method and optimization of the catalytic performance for methanol electro-oxidation. The investigation indicates that the GRR method utilizes the different reduction potentials between the precursor element and Pt substances as resultant in the Au core is completely covered by uniformly grown Pt shell. K. Shim et al. [26] have successfully the synthesised core-shell Au-Pt nanoparticles using the ultrasonic irradiation approach and examined the glucose oxidation reaction. The results demonstrate that the Au@Pt nanoparticles can be utilized as the efficient glucose sensor in neutral solution with a detection limit of (319.8 ± 5.4) nM. Hu-Jun Lee et al. [39] report the growth mechanism of Pt shells on the Au core at low Pt precursor concentrations with the aid of co-reduction and ultrasonication. This investigation highlights the critical role of ultrasonication and its effect on the formation mechanism of Au@Pt core–shell nanoparticles. Y. Mizuno et al. [22] study the synthesis of the Au@Pt core-shell nanoparticles by sonochemical reduction and chemical reduction in the presence of a non-ionic surfactant and ultrafine bubbles (UFBs). The catalytic activity indicates that the Au@Pt NPs synthesized with UFBs exhibited high catalytic performance for the reduction of 4-notrophenol. Ribing Cao et al. [31] report a facile seed-mediated growth method, in which Pt shell are grown on the Au core by using ascorbic acid (AA) as reducing reagents. The influence of AA reduction time on the morphology of Au@Pt NPs is investigated. The Au@Pt NPs prepared at the AA reduction time of 4h reveals the highest catalytic performance for the methanol oxidation. Yijing Li and co-workers [35] report a facile and efficient method for high yield synthesis of Au@Pt NPs via the overgrowth of Pt shell on in situ gold core in aqueous media, resulting in Au@Pt NPs with sizes of about 14 nm. The reaction conditions such as an incubation time of $HAuCl_4$ solution, a mixing time of $HAuCl_4$ and K_2PtCl_4 solution and molar ratios of Au/Pt are optimized to obtain the high catalytic performance.

For the consideration of both economy and environment, a facile and green approach to fabrication high yield and controlled core-shell nanoparticles is our purposes. In current study, we developed a novel and green approaches to synthesis core-shell Au-Pt nanoparticles. Au nanoparticles (AuNPs) are first prepared via the well-established method [40, 41]. Pt shell is then grown on the Au nanoparticles in the absence of surfactant agents at room temperature. Leaves extraction is a green and clean reductant, is served to reduce K_2PtCl_6. The structure, morphology, and composition of the obtained Au@Pt NPs are characterized by FE-SEM, XRD, UV-Vis and DLS. The result illustrate that Au@Pt NPs has been successfully synthesized. The influence of the atomic ratio between Au and Pt on the formation mechanism of the Au@Pt NPs is investigated. Interestingly, the Au@Pt NPs generated at ratio of 1:1 exhibits good morphology, homogeneity in size and stability on the gold nanoparticles (AuNPs) in comparison with the other synthesized Au@Pt NPs.

2. Experimental

2.1. Materials and Chemicals

In the present study, the reagents including gold (III) chloride trihydrate ($HAuCl_4$. $3H_2O$, ≥ 99,9%), chloroplatinic acid hexahydrate ($H_2PtCl_6.6H_2O$, ≥ 99,9%) and ethanol (CH_3CH_2OH, ≥ 99,5%) are obtained from Sigma-Aldrich (Sigma-Aldrich, St. Louis, MO, USA) and directly used without any additional purification. Dried green tea leaves are purchased from a local supermarket. Deionized (DI) water (18.2 $M\Omega\ cm^{-1}$) is produced using a system equipped with an Ultra RS-U20i and used in all experiments. All the glassware containers are washed with deionized water and ethanol before the experiments.

2.2. Preparation of green tea leaves extract

The dried green tea leaves are grinded to obtain fine leaves powders. The green tea extract is prepared as follows: 100 mg powders of dried green tea leaves are weighted and put in a 250 ml beaker contains a mixture of 150 ml DI water and 50 ml ethanol. Afterward, the green tea leaves and solvent mixtures are heated at 80°C for 120 min. The hot mixtures are cooled to room temperature and filtered using a filter paper. A yellow color aqueous extract of green tea leaves is obtained and utilized for the synthesis of gold-platinum nanoparticles.

2.3. Synthesis of gold-platinum core-shell nanoparticles using green tea leaves extracts.

Gold (III) chloride trihydrate and chloroplatinic acid hexahydrate are used as the gold and platinum precursors. The $HAuCl_4$ and H_2PtCl_6 separately dissolute in DI water in order to obtain an aqueous solution at a concentration of 10 mM.

The synthesis of gold nanoparticles using green tea leaves extract is to be the reduction of Au^{3+} to Au^0 and briefly described as follows: 20 ml aqueous extracts of the green tea leaves are heated at 60°C for 15 min. Afterward, 1 ml of 10 mM Au^{3+} aqueous solution is added. The reaction mixtures are heated at

60°C and vigorously stirred by the magnetic stirrer for 30 min. The mixtures are changed in coloration from a yellow colour to a purple colour, indicating the formation of gold nanoparticles and labelled as AuNPs.

A typical procedure for the synthesis of gold-platinum core-shell nanoparticles with Au/Pt molar ratio = 1:1 (Au@Pt (1:1)) is given as follows. 20 ml aqueous extracts of the green tea leaves utilized a reducing and capping agent are heated at 60°C and stirred by the magnetic stirrer. Afterward, 1 ml of 10 mM aqueous $HAuCl_4$ solution is added dropwise into 20 ml of the green tea leaves extract. This reaction mixture including a green tea extract and $HAuCl_4$ aqueous solution is continued to heat and under vigorously stir for the reduction of gold ions at 60°C for 30 min. The coloration of reaction mixture is changed from pale yellow color to a purple color within a several minutes visually confirms the formation of gold nanoparticles (AuNPs). For Au@Pt core-shell nanoparticles, 1 ml of 10 mM aqueous H_2PtCl_6 solution is introduced into the gold nanoparticles solution under vigorous magnetic stirring at 60°C. After 3 hours, the black solution is obtained, which demonstrate that the core-shell Au-Pt nanoparticles are generated. At the end of the procedure, the resultant nanoparticles samples are washed with DI water by centrifuging at 10000 rpm for 1h to remove an excess of reactants from the suspensions. At the end of the centrifuging, the prepared resultant Au@Pt nanoparticles are dispersed in 1 ml of DI water for further characterization.

In this work, we synthesized Au-Pt core-shell structures with different Au:Pt molar ratios of 2:1, 1:1 and 1:2 and denoted as Au@Pt (2:1), Au@Pt (1:1), Au@Pt (1:2), respectively. For the synthesis of the Au@Pt (1:2) and Au@Pt (2:1) samples, the volumetric of $HAuCl_4$ aqueous solution is fixed to 1 ml, while the volumetric of aqueous H_2PtCl_6 solution is to be of 2.0 and 0.5 ml, respectively. All the other experiment conditions are the same.

2.4. Characterization techniques

Field emission scanning electron microscopy instrument (FE-SEM, Hitachi SU8010, Japan) are used at acceleration voltages of 20 kV to study nanostructure of synthesized Au@Pt NPs samples, including size, shape and surface morphology. The FE-SEM samples are prepared by dropping Au@Pt NPs solution on the surface of a carbon tape and dried well at room temperature.

UV-Vis absorption spectra of the nanoparticles are collected in the wavelength number from 400 to 800 nm at room temperature by a Carry 100 spectrophotometer.

X-Ray diffraction (XRD) measurement are carried out on a D8 Advance Eco, Bruker AXS spectrometer (Germany) using Cu-Kα radiation (λ = 0.1542 nm), operated at a voltage of 40 kV, a current of 10 mA and a scan rate of 2° min^{-1} commencing 30° to 90°.

The particle size distribution of the Au@Pt NPs is measured by Dynamic light scattering (DLS) equipment (Horiba LB-550) with 4 mW He-Ne at 633 nm.

3. Results and discussions

Figure 1 depicts the experimental procedure applied to synthesis Au@Pt NPs using green tea leaves extracts as reducing and a capping reagent. The nanoparticles are synthesized in aqueous solution by chemical reduction method. It is well known that lattice parameters of Gold and Platinum are similar with Au being slenderly higher in size [7]. The surface energies (fcc (111)) of Pt and Au are to be 2.35 m^{-2} and 1.61 Jm^{-2}, respectively, and strongly depend on the environment [7].

According to previous studies [35, 37, 40], the Au^{3+} ion solutions are preferentially reduced to Au atom in green tea leaves extract to obtain Au nanoparticles. Subsequently, the Pt^{6+} ion solutions are reduced by green tea leaves extract to obtain the Au@Pt nanoparticles [15, 22, 23, 27]. After the synthesis of nanoparticles, the green tea leaves extracts cover the surface of nanoparticles and act as surfactant to stabilize NPs in solution.

UV-visible spectroscopy of Au@Pt NPs

In this study, the core-shell Au-Pt nanoparticles are synthesized using green tea leaves extracts. According to literature review, the green tea extracts exhibit the presence of polyphenol, and flavonoids compounds, which can be used as reducing and stabilizing agents for nanoparticle synthesis [33, 35]. Because the reduction potential of gold ions (Au^{3+}) is higher than that of Pt^{+6}, the Au nanoparticles are firstly obtained by reduction of $HAuCl_4$ into Au atoms (Au^0) as reported by [8, 9, 14, 15]. We can see a change in color of Au^{3+} solutions from light yellow to ruby red color of Au nanoparticles after addition of green tea leaves extracts. Subsequently, H_2PtCl_6 was reduced by green tea leaves extracts. During the progress of H_2PtCl_6 reduction, the solution color is easily observed, the purple color of the gold solution is gradually turned black over the course of 3 h, indicating that Pt shell is deposited on AuNPs core surface. The optical properties of AuNPs and Au@Pt NPs are investigated by the UV-vis spectrometer measurements. The optical absorption of AuNPs and Au@Pt NPs exhibit their localized surface plasmon resonances (LSPR) because the oscillation of conduction electrons is associated with the incident electromagnetic wave [17, 27–29].

Figure 2 illustrates UV-vis absorption spectra of the AuNPs and Au@Pt NPs synthesized with different molar ratios of Au and Pt (2:1, 1:1 and 1:2). As can be seen in Fig. 2(B), the UV-Vis spectrum of Au nanoparticles shows the absorption peak at λ_{max} = 540 nm, which are consistent with the previous report by K. Yasuda et al. [33]. According to previous reports by [35, 37, 39], the Pt nanoparticles exhibit two absorption peaks at 216 and 264 nm. After growth of Pt shell on Au core, the SPR absorption spectra at 540 nm are shifted to lower wavelength of 530, 528 and 521 nm corresponding to the different Au:Pt molar ratios of (2:1), (1:1) and (1:2), respectively. In addition, the Au@Pt NPs display a decrement in the absorption peaks and a characteristic of a small and weak absorption bands can be clearly identified as indicated in the Fig. 2 (C). On the other hand, the Pt shell is successfully grown on AuNPs surface and evidenced by the shift in SPR wavelength from 540 nm (AuNPs) to 520–530 nm (Au@Pt NPs), which is

agreement with the previous reports [27–29]. The thickness of Pt shell is thin and calculated from FE-SEM measurements (Table 1). To further confirm the growth of Pt shell, the ruby red colour of AuNPs solution is progressively changed into dark brown colour with different Au:Pt molar ratios as demonstrated in the Fig. 2 (A). These results have provided evidence that the platinum shell is grown on the surface of Au nanoparticles [15, 24, 26]. Furthermore, the surface morphologies and crystalline structure of the nanoparticles are investigated by using FE-SEM and XRD measurements in order to ascertain the core-shell structure of Au-Pt synthesized using green tea leaves extract.

Field emission scanning electron microscopy (FE-SEM)

FE-SEM images of the AuNPs and Au@Pt NPs synthesized with different Au:Pt molar ratios of 2:1, 1:1 and 1:2, as shown in the Fig. 3 and Fig. 4, reveal surface morphology, shape and particle size. According to Fig. 3(a), it is clear that the FE-SEM images of the AuNPs display uniform, smooth spherical shapes without any agglomeration. The average particle sizes of Au nanoparticles are determined to be 18.4 nm. The surface morphologies of the spherical Au nanoparticles are significantly changed after the reduction of Pt precursor in green tea leaves extract, resulting formation of Au@Pt core-shell nanoparticles. It can be seen in Fig. 3 and Fig. 4, the particle sizes of Au@Pt nanoparticles are effectively changed due to varying the molar ratios of Au and Pt (2:1, 1:1, 1:2). The platinum layer is grown on the surface of the Au nanoparticles, resulting in the particle sizes of the Au@Pt NPs would be greater in comparison with the original AuNPs [22, 23]. The difference in the particle size is associated with the thickness of the Pt shell. According to the FE-SEM images shown in Fig. 3 and Fig. 4, the average particle sizes of the Au@Pt (2:1), Au@Pt (1:1) and Au@Pt (1:2) are calculated to be 22.5, 26.7 and 50.8 nm, respectively, which are 4.2, 8.3 and 12.4 nm greater compared with the AuNPs nanoparticle size of 18.4 nm, indicating a progressive increase in shell thickness. Importantly, in Fig. 3(b), the FE-SEM images of Au@Pt (2:1) reveal that the Au@Pt nanoparticles are still maintained the spherical shape and smooth surface after growth of Pt layer. As shown in Fig. 4 (a), the FE-SEM images of the Au@Pt (1:1) demonstrate a slightly uneven surface and inhomogeneous distribution of Pt shell, possibly reflecting the granular nature of Pt [4, 7, 13]. The brightened contrast areas are observed in the FE-SEM images due to the rich in Pt content. The surface roughness of Au@Pt (1:1) sample clearly demonstrated the growth of Pt layer. These observations are consistent with those from report R. Cao et al. [31]. They prepared core-shell Au-Pt nanoparticles using acrobic acid (AA), which acted as surfactant agents. The FE-SEM results show that spherical Au nanoparticles coated with Pt shell are clearly observed in the higher magnification image. Au and Pt are observed in the EDX spectrum, indicating that the Au and Pt precursors are reduced in acrobic acid and that Pt shell grew on the Au core surfaces, forming a core-shell structure. In Fig. 4 (b), it is difficult to distinguish between Au core and Pt shell because the FE-SEM image of the Au@Pt (1:2) does not exhibit a different contrast of Au and Pt. Table 1 summarizes the measurements of Au@Pt NPs sizes and Pt shell thickness.

The formation mechanism of Pt shell can be explained as follows [23]: As soon as addition of the H_2PtCl_6 aqueous solution, the galvanic replacement reaction starts tacking place to reduce the Pt precursor in to Pt^0 randomly on Au core surface. The migration of vacancies and the gradual formation

of voids are created by the growth of Pt precipitates. As results, the uniform deposition of Pt^0 is observed on the surface of nanoparticles in a granular morphology.

Table 1
The average particles size and average shell thickness of the Au@Pt NPs synthesized with different molar ratios of Au and Pt, from FE-SEM and DLS measurements.

Samples	Average particle size and shell thickness from FE-SEM		Average particle size from DLS	UV-Vis measurement, λ_{max} (nm)
	Average particle size (nm)	Average shell thickness (nm)		
AuNP	18.4	N/A	21.6	540
Au@Pt (2:1)	22.5	4.1	27.4	530
Au@Pt (1:1)	26.7	8.3	36.8	528
Au@Pt (1:2)	50.8	32.4	102.1	521

Dynamic light Scattering (DLS)

Dynamic light scattering (DLS) method is well known based on the measuring time - dependent fluctuations in scattered light intensity caused by the Brownian movement of nanoparticles [13–15]. In order to further understand the particle size distribution, DLS measurements are performed on the AuNPs and Au@Pt NPs synthesized with three different Au:Pt molar ratios of 2:1, 1:1, 1:2 as shown Fig. 5. It is in evidence that both AuNPs and Au@Pt NPs exhibit narrow size distribution, the particle size is majorly distributed in the range of 10–20 nm, 20–30 nm, 30–40 nm and 100–110 nm for the AuNPs, Au@Pt (2:1), Au@Pt (1:1) and Au@Pt (1:2), respectively. The average particle size of the AuNPs, Au@Pt (2:1), Au@Pt (1:1) and Au@Pt (1:2) is evaluated to be 21.6, 27.4, 36.8 and 102.1 nm, which is greater than that FE-SEM measurements. The comparison of average particle size between FE-SEM and DLS measurements is summarized in Table 1. These results confirm once again that as the molar ratios of Au and Pt decreased, the particle sizes became larger.

X-Ray diffraction analysis of Au/Pt core-shell nanoparticles

The crystaline structure of the AuNPs and Au@Pt nanoparticles is obtained by XRD. The XRD survey spectrum of Au@Pt NPs with different molar ratios of Au and Pt (2:1, 1:1 and 1:2) are illustrated in Fig. 6. As seen in Fig. 6, the XRD patterns of AuNPs exhibit the sharp and intense diffraction peaks at 2θ values of 38.2°, 44.4°, 64.6°, and 77.6°, corresponding to the diffraction planes (111), (200), (220), and (311) reflections of the Au fcc structure (JCPDF 04-0784), respectively [16, 17, 20]. The XRD patterns of Au@Pt NPs illustrate that the peaks at 2θ values of 38.3°, 44.2°, 64.5°, and 77.6°, which is described to (111), (200), (220), and (311) crystalline planes of the Au fcc structure, respectively, and at 39.6°, 46.2°, 67.5°

which are related to (111), (200), and (220) crystalline planes of the Pt fcc structure (JCPDF 04-0802), respectively [26–28].

Important to mention that the XRD patterns show reflections corresponding to the peak positions of Au and Pt. All diffraction peaks in the XRD pattern of the Au@Pt NPs are matched to a face-centered cubic structure of Au and Pt with lattice parameter values of 0.4078 nm and 0.3926 nm for Au and Pt, respectively, compared to their pure counterpart based on available literature, confirming the formation of core-shell Au-Pt nanoparticles [21. The intensity of diffraction peaks is dependent on the Au:Pt molar ratios, suggesting the crystalline phases of gold and platinum are mainly structure of the Au@Pt NPs. The detail of the [111] diffraction of Au and Pt crystalline structure is indicated in Fig. 6**(e).** In comparison to the Au reflections, the Pt reflections exhibit a low intensity and wide shape, suggesting the size of Pt crystallites is much smaller than that of Au crystallites. It is clear that the diffraction peak intensity of Pt increases by varying the molar ratios between Au and Pt from (2:1) to (1:2), indicating the thickness of Pt shell on the Au nanoparticles can be effectively controlled. These results confirm that the core-shell nanoparticles of Au and Pt reveal the Pt shell with different thickness. These results are in good agreement with the previous report by Yuki Mizuno et al. [22], they reported that the face centered cubic structures of both gold and platinum are detected in X-Ray diffraction, indicating that the core-shell Au-Pt nanoparticles are successfully prepared by chemical reduction.

4. Conclusions

In the current study, we have synthesized the core-shell Au-Pt nanoparticles (Au@Pt NPs) by chemical reduction method using green tea leaves extracts as stabilizing and a reducing agent. The surface morphologies, average particle size, crystalline structure and optical properties of the synthesized Au@Pt NPs are characterized by a comprehensive set of measurements including FE-SEM, UV-Vis, DLS and XRD. Combined with the results of FE-SEM and XRD measurements, the Au@Pt NPs are successfully synthesized. The thickness of Pt shell on the Au core can be effectively controlled by varying the molar ratios of Au:Pt. This work provides a new, facile and efficient synthetic approach for the preparation of core-shell Au-Pt nanoparticles.

Declarations

Acknowledgments The authors acknowledge the financial support from Vietnam National University Ho Chi Minh City (VNUHCM) under grant number 562-2024-32-01.

Author contribution Le Thi Mai Hoa: Conceptualization, methodology, measurement, formal analysis, investigation, original manuscript preparation, writing-review and editing, visualization, project administration.

Funding This research was funded by Vietnam National University Ho Chi Minh City (VNUHCM) under grant number 562-2024-32-01.

Data availability No datasets were generated or analyzed during the current study.

Conflict of interests The authors declare that have no conflict of interests.

References

1. Cai B, Henning S, Herranz J, Schmidt T J, Eychmüller A (2017) Nanostructuring noble metals as unsupported electrocatalysts for polymer electrolyte fuel cells. Adv. Energy Mater. **7:** 1700548.
2. Li G, Kanezashi M, Tsuru T (2017) Catalytic ammonia decomposition over high peformance Ru/graphene nanocomposites for efficient COx-free hydrog production. Catalysts **7(1)**: 23.
3. Tang H, Su Y, Chi B, Zhao J, Dang D, Tian X, Liao S, Li G R (2021) Nodal PtNi nanowires with Pt skin and controllable Near-Surface composition for enhanced oxygen reduction electrocatalysis in fuel cells. Chem. Eng. J. **418:** 129322.
4. Li Y, Ding W, Li M, Xia H, Wang D, Tao X (2015) Synthesis of core–shell Au–Pt nanodendrites with high catalytic performance via overgrowth of platinum in situ gold nanoparticles. J. Mater. Chem. A **3:** 368–376.
5. Guo Z, Zhang X, Sun H, Dai X, Yang Y, Li X, Meng T (2014) Novel honeycomb nanosphere Au@Pt bimetallic nanostructure as a high performance electrocatalyst for methanol and formic acid oxidation. Electrochimica Acta **134**: 411–417.
6. Jia H, Chang G, Shu H, Xu M, Wang X, Zhang Z, Liu X, He H, Wang K, Zhu R, He Y (2017) Pt nanoparticles: facile synthesis and enhanced electrocatalytic performance for methanol oxidation. J. Hydrogen Energy **42:** 22100–22107.
7. Higareda A, Kumar-Krishna S, García-Ruiz A F, Maya-Cornejo J, Lopez-Miranda J L, Bahena D, Rosas G, Pérez R and Esparza R (2019) Synthesis of Au@Pt Core-Shell Nanoparticles as efficient electrocatalyst for Methanol Electro-Oxidation. Nanomaterials **9:** 1644.
8. Duan M Y, Liang R, Tian N, Li Y J, Yeunga E S (2013) Self-assembly of Au–Pt core-shell nanoparticles for effective enhancement of methanol electrooxidation. Electrochimica Acta **87:** 432-437.
9. Iyyamperumal R, Zhang L, Henkelman G, Crooks R M (2013) Efficient electrocatalytic oxidation of formic acid using Au@Pt dendrimer-encapsulated nanoparticles. J. Am. Chem. Soc. **135:** 5521-5524.
10. Zhang C, Zhu A, Huang R, Zhang Q, Liu Q (2014) Hollow nanoporous Au/Pt core–shell catalysts with nanochannels and enhanced activities towards electro-oxidation of methanol and ethanol. Int. J. Hydrogen Energy **39:** 8246–8256.
11. Coccia F, Tonucci L, Bosco D, Bressan M and d'Alessandro N (2012) One-pot synthesis of lignin-stabilised platinum and palladium nanoparticles and their catalytic behaviour in oxidation and reduction reactions. Green Chemistry **14**: 1073-1078.
12. Chen A, Holt-Hindle P (2010) Platinum-based nanostructured materials: synthesis, properties, and applications. Chem. Rev. **110:** 3767-3804.

13. Lee H J, Hanyu D, Dao N A T, Kasai H, Suzuki M, Yabu H, Nakatani H, Kaneko K (2024) Controlling the composition and nanostructure of Au@Ag–Pt core@multi-shell nanoparticles prepared by co-reduction method. Materials Today Chemistry **38(7):** 102132
14. Gawande M B, Goswami A, Asefa T, Guo H, Biradar A V, Peng D L, Zboril R and Varma R S (2015) Core–shell nanoparticles: Synthesis and applications in catalysis and electrocatalysis. Chem. Soc. Rev. **44**: 7540-7590.
15. He L L, Zheng J N, Song P, Zhong S X, Wang A J, Chen Z, Feng J J (2015) Facile synthesis of platinum-gold alloyed string-bead nanochain networks with the assistance of allantoin and their enhanced electrocatalytic performance for oxygen reduction and methanol oxidation reactions. J. Power Sources **276**: 357-364.
16. Mourdikoudis S, Chirea M, Zanaga D, Altantzis T, Mitrakas M, Bals S, Liz-Marzán L M, Pérez-Juste J, Pastoriza-Santos I (2015) Governing the morphology of Pt-Au heteronanocrystals with improved electrocatalytic performance. Nanoscale **7**: 8739-8747.
17. Kartashova A D, Gonchar K A, Chermoshentsev D A, Alekseeva E A, Gongalsky M B, Bozhev I V, Eliseev A A, Dyakov S A, Samsonova J V, Osminkina L A(2022)Surface-enhanced Raman scattering-active gold-decorated silicon nanowire substrates for label-free~~m~~detection of bilirubin. ACS Biomater. Sci. Eng. **8**: 4175–4184.
18. Song H M, Anjum D H, Sougrat R, Hedhili M N, Khashab N M (2012) Hollow Au@Pd and Au@Pt core-shell nanoparticles as electrocatalysts for ethanol oxidation reactions. J. Mater. Chem. **22:** 25003-25010.
19. You H, Zhang F, Liu Z, Fang J (2014) Free-standing Pt-Au hollow nanourchins with enhanced activity and stability for catalytic methanol oxidation. ACS Catal. **4:**2829-2835.
20. Gharibshahia E, Saion E, Luigi Johnston R, Ashraf A (2019) Theory and experiment of optical absorption of platinum nanoparticles synthesized by gamma radiation. Applied Radiation and Isotopes **147:** 204-210.
21. Nuti S, Fernández-Lodeiro J, Palomo J M, Capelo-Martinez J L, Lodeiro C and Fernández-Lodeiro A (2024) Synthesis, Structural Analysis, and Peroxidase-Mimicking Activity of AuPt Branched Nanoparticles, Nanomaterials **14**:1166.
22. Mizuno Y, Yamamoto Y, Yamaguchi T, Yasuda K (2025) Size control of Au@Pt core-shell nanoparticles for enhanced catalytic activity using ultrafine bubbles and ultrasound, Japanese Journal of Applied Physics **64**: 03SP32.
23. Takeuchi Y, Lee H J, Dao A T N, Kasai H, Teranishi R, Kaneko K (2021) Formation of multishell Au@Ag@Pt nanoparticles by coreduction method: a microscopic study. Materials Today Chemistry **21:** 100515.
24. Quang T A, Tran T M C, Aminabhavi T M, Gnanasekaran L, Vasseghian Y, Joo S W (2025) Chiral plasmonic Au@Pt nanoparticles for detection of H_2O_2 and Hg^{2+} and enantiomeric differentiation. Journal of Environmental Management **373**: 123561.

25. Dorjgotova A, Jeona Y, Hwanga J, Ulziidelgera B, Su Kim H, Hana B, Shula Y G (2017) Synthesis of Durable Small-sized Bilayer Au@Pt Nanoparticles for High Performance PEMFC Catalysts. Electrochimica Acta **228**: 389–397.
26. Shim K, Lee W C, Park M S, Shahabuddin M, Yamauchi Y, Hossain M S A, Shim Y B, Ho Kim J (2019) Au Decorated Core-Shell Structured Au@Pt for the Glucose Oxidation Reaction. Sens. Actuators B Chem. **278:** 88–96.
27. Su S, Zhang C, Yuwen L, Liu X, Wang L, Fan C, Wang L (2016) Uniform Au@Pt core-shell nanodendrites supported on molybdenum disulfide nanosheet form ethanol oxidation reaction. Nanoscale **8:** 602–608.
28. Feng R, Li M, Liu J (2012) Synthesis of core–shell Au@Pt nanoparticles supported on Vulcan XC-72 carbon and their electrocatalytic activities for methanol oxidation. Colloids and Surfaces A: Physicochem. Eng. Aspects **406:** 6-12
29. Cui Q, Shen G, Yan X, Li L, Mohwald H, Bargheer M (2014) Fabrication of Au@Pt multibranched nanoparticles and their application to in situ SERS monitoring. ACS Appl. Mater Interfaces **6:** 17075-17081.
30. Zhou G, Xu Y, Fu Y, Yang Y, Zhang Y (2014) Surfactant-free synthesis of carbon-Supported Au@Pt nanocatalysts for methanol oxidation. Int. J. Electrochem. Sci. **9:** 3990-3999.
31. Cao R, Xia T, Zhu R, Liu Z, Guo J, Chang G, Zhang Z, Liu X, He Y (2018) Novel synthesis of core-shell Au-Pt dendritic nanoparticles supported on carbon black for enhanced methanol electro-oxidation, Applied Surface Science **433**: 840-846
32. Yan S, Zhang S, Zhang W, Li J, Gao L, Yang Y, Gao Y (2014) Application of carbon supported Pt core–Au shell nanoparticles in methanol electro oxidation, J. Phys. Chem. C **118**: 29845-29853.
33. Yasuda K, Sato T, and Asakura Y (2020) Size-controlled synthesis of gold nanoparticles by ultrafine bubbles and pulsed ultrasound, Chem. Eng. Sci. **217**:115527.
34. Azuma Y and Yamamoto K (2024) Effects of destruction of Euglenagracilis by ultrasonic cavitation, Jpn. J. Appl. Phys. **63:** 02SP89.
35. Li Y, Ding W, Li M, Xia H, Wang D, Tao X (2015) Synthesis of core-shell Au-Pt nanodendrites with high catalytic performance via overgrowth of platinum on in situ gold nanoparticles. J. Mater. Chem. A. **3:** 368-376
36. Brosseau Q, Usabiaga F B, Lushi E, Wu Y, Ristroph L, Zhang J, Ward M, Shelley M J (2019) Relating rheotaxis and hydrodynamic actuation using asymmetric gold-platinum phoretic rods, Phys. Rev. Lett. **123**: 178004-178005.
37. Banerjee V, Kumaran V, Santhanam V (2015) Synthesis and characterization of Au@Pt nanoparticles with ultrathin platinum over layers. J. Phys. Chem. C **119:** 5982–5987.
38. Hansen H E, Seland F, Sunde S, Burheim O S, Pollet B G (2022) Frequency controlled agglomeration of pt-nanoparticles in sonochemical synthesis. Ultrasonics Sonochemistry **85:**105991.
39. Lee H J, Hanyu D, Ngoc Dao AT, Kaneko K (2025) Insights into the formation of Au@Pt dendritic core–shell nanoparticles with the aid of ultrasonication, Scientific Reports **15**: 29474.

40. Zhang G, Zheng H, Shen M, Wang L, Wang X (2015) Green synthesis and characterization of Au@Pt core–shell bimetallic nanoparticles using gallic acid, Journal of Physics and Chemistry of Solids **81:** 79–87.
41. Ramli N H, Nor N M, Abu Bakar A H, Zakaria N D, Lockman Z, Abdul Razak K (2024) Platinum-based nanoparticles: A review of synthesis methods, surface functionalization, and their applications. Microchemical Journal **200**:110280.

Figures

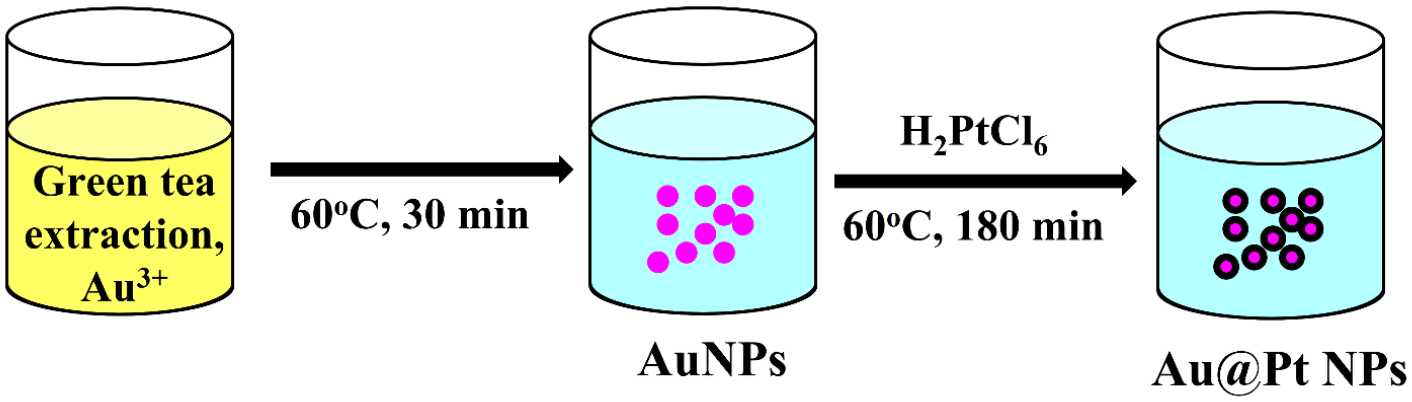


Figure 1

Schematic illustration of a facile and environmentally friendly method of the synthesis of core-shell Au-Pt nanoparticles using green tea leaves extracts.

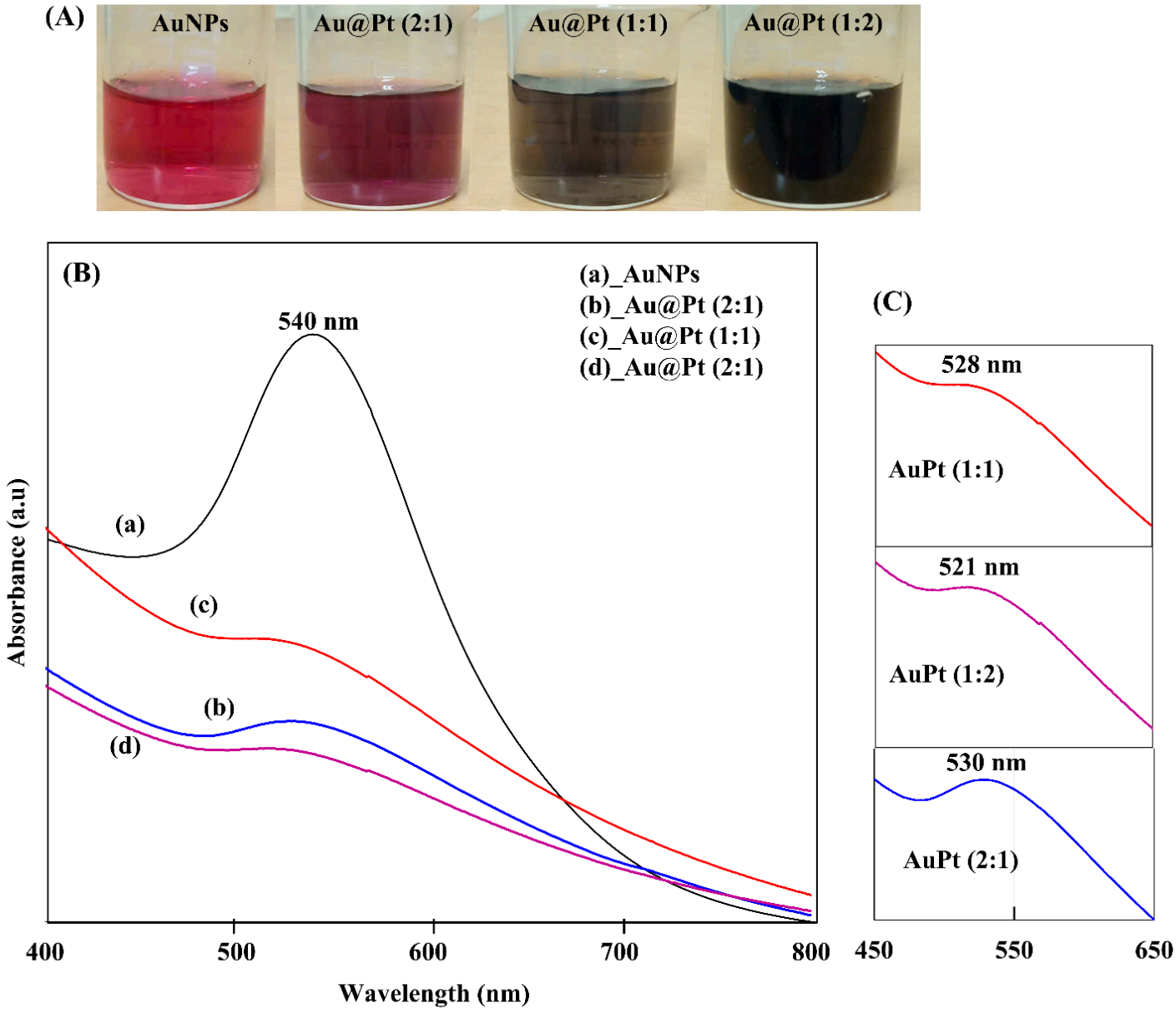


Figure 2

(A) Digital photographs of AuNPs and Au@Pt core-shell nanoparticles with different Au:Pt molar ratios, (B, C) UV-Visible absorption spectra of AuNPs and Au@Pt NPs synthesized with different molar ratios of Au and Pt.

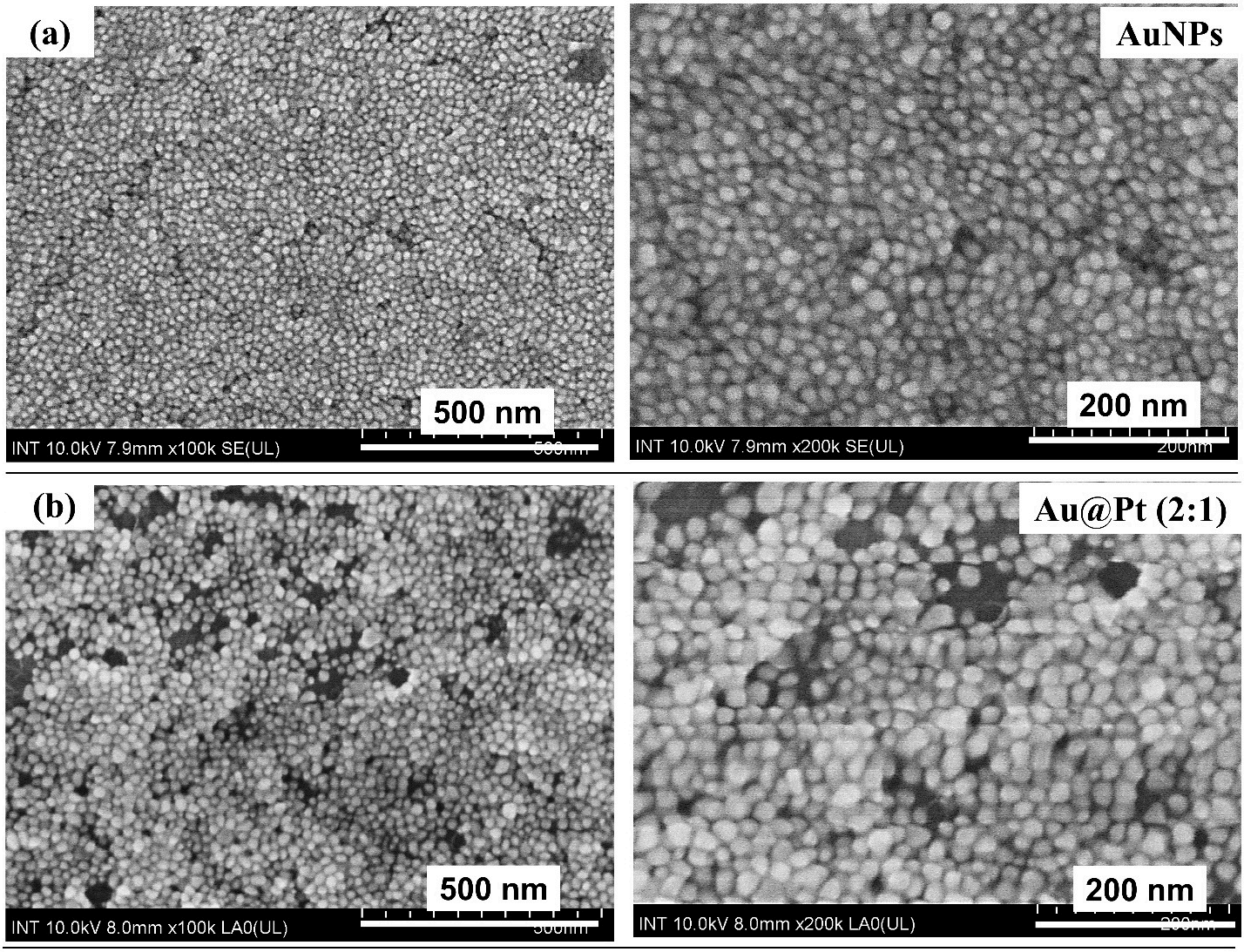


Figure 3

FE-SEM images of: (a) AuNP and (b) Au@Pt (2:1) nanoparticles synthesized with Au:Pt molar ratios of 2:1

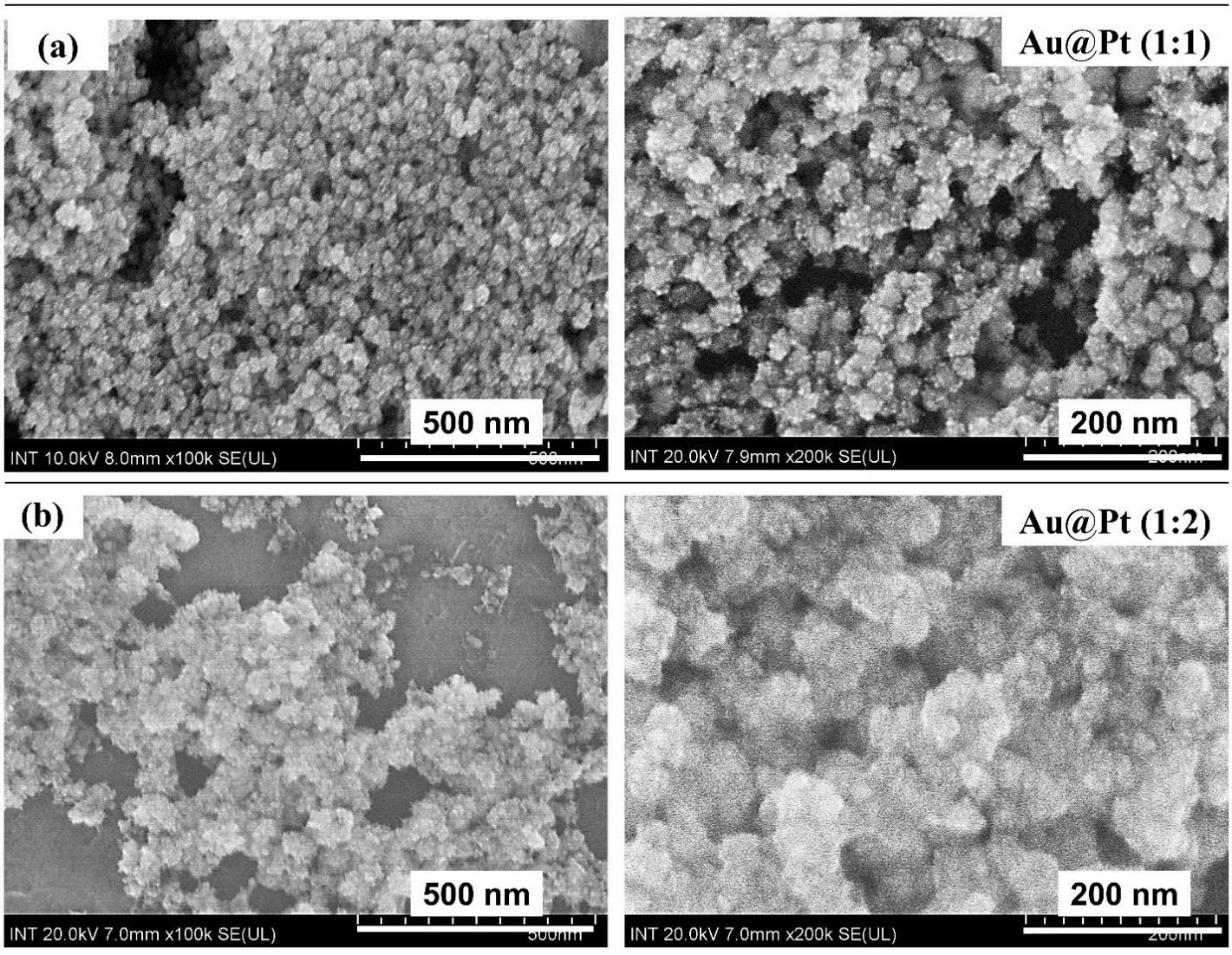


Figure 4

FE-SEM images of the Au@Pt nanoparticles synthesized with different Au:Pt molar ratios: (a) Au@Pt (1:1) and (b) Au@Pt (1:2).

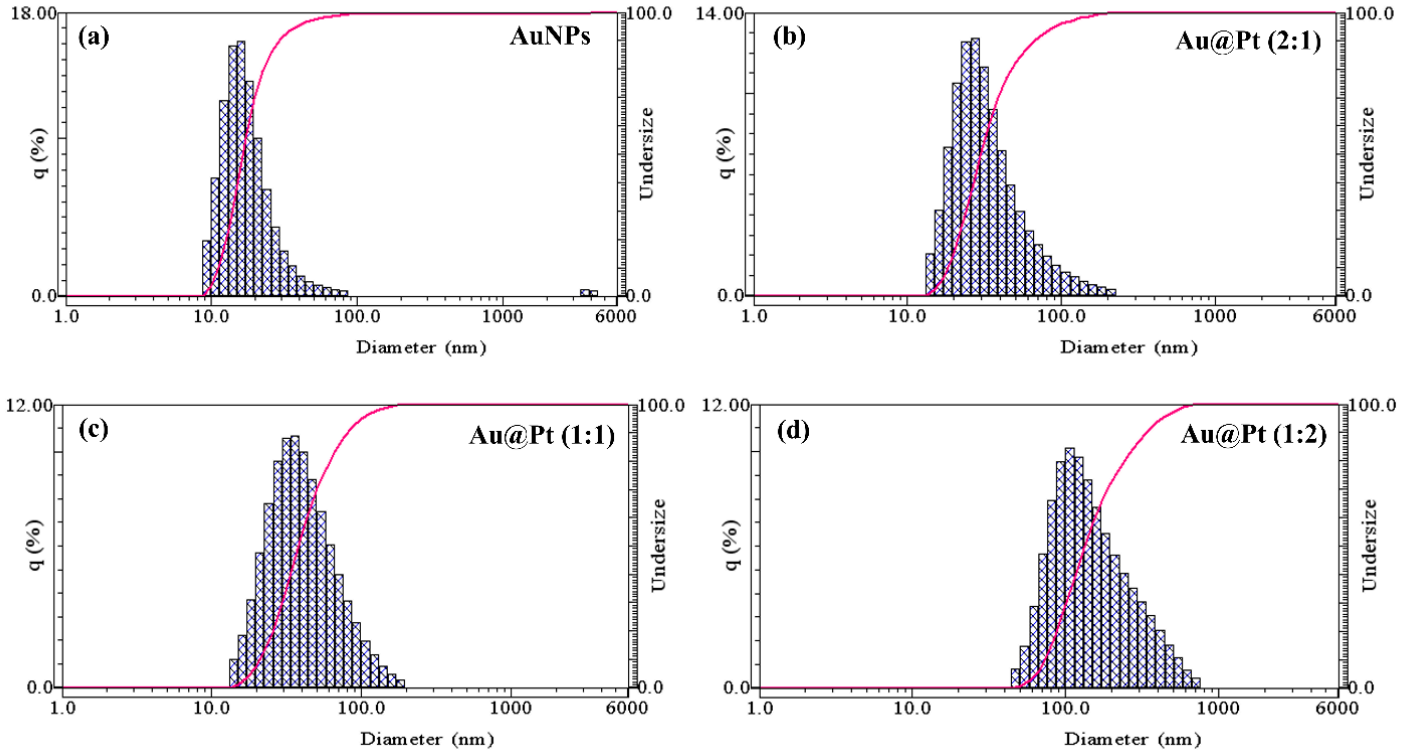


Figure 5

Size distribution measured by DLS of: (a) AuNPs and Au@Pt nanoparticles synthesized with different Au:Pt molar ratios: (b) Au@Pt (2:1), (c) Au@Pt (1:1), (d) Au@Pt (1:2)

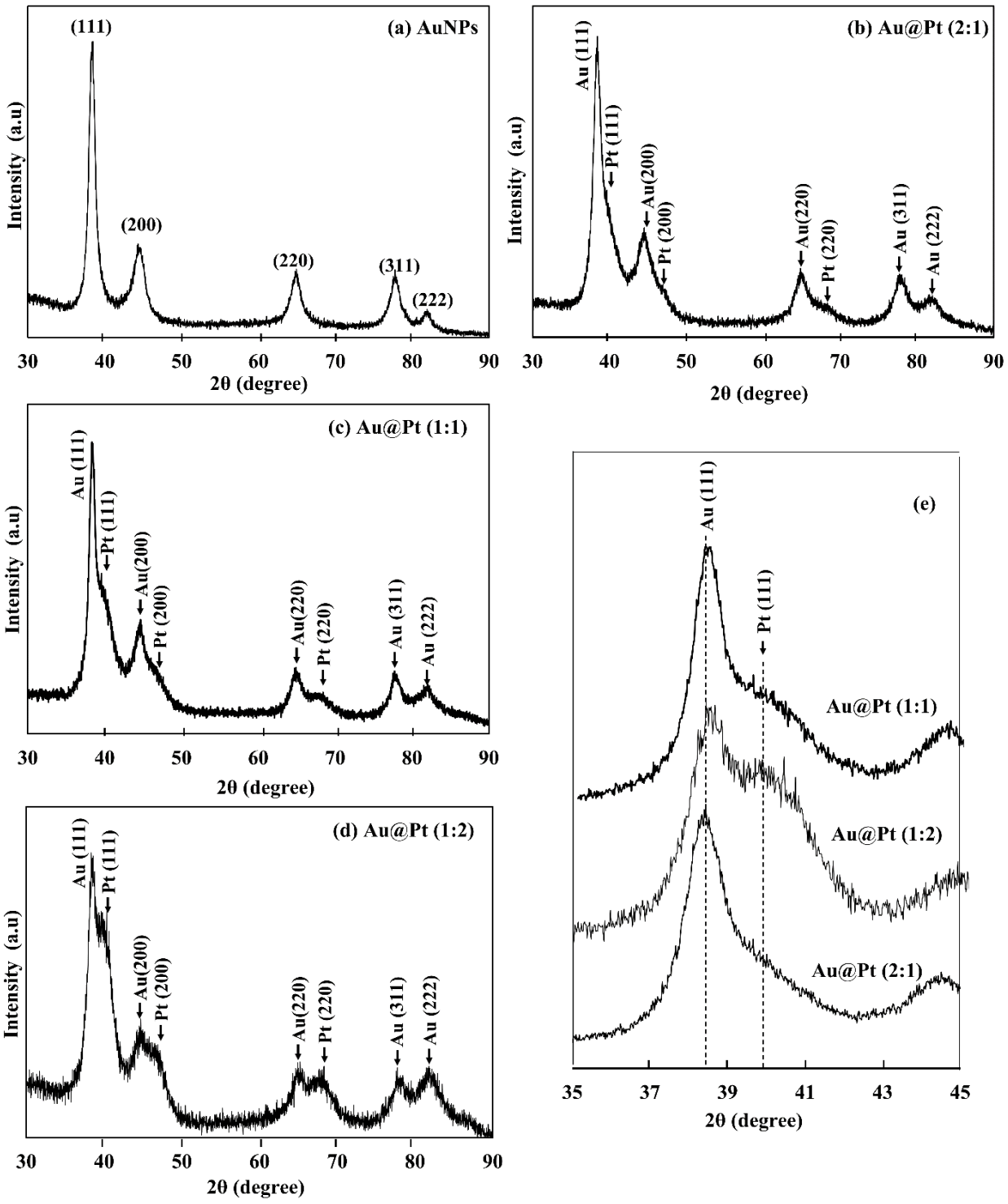


Figure 6

X-ray diffraction patterns of: (a) AuNPs and Au@Pt nanoparticles synthesized with different Au:Pt molar ratios: (b) Au@Pt(2:1), (c) Au@Pt(1:1), (d) Au@Pt(1:2) and (e) (111) reflection of Au and Pt structures.